

Hall-effect characterization of electron transport at SiO₂/4H-SiC MOS interfaces

G.A. Umana-Membreno^{a,1}, S. Dhar^b, A. Choudhary^a, S.-H. Ryu^c, J. Antoszewski^a, L. Faraone^a

^a*School of Electrical, Electronic & Computer Eng., The University of Western Australia, Crawley WA 6009, Australia*

^b*Physics Department, Auburn University, Auburn, AL 36849, U.S.A.*

^c*Cree, Inc., 4600 Silicon Drive, Durham, NC 27703, U.S.A.*

Abstract

Magnetic-field dependent resistivity and Hall-effect measurements combined with high resolution mobility spectrum analysis (HR-MSA) were employed to study room-temperature electronic transport in 4H-SiC metal-oxide-semiconductor field-effect transistor (MOSFET) structures. It is shown that the mobility distribution for electrons at the SiO₂/SiC interface is significantly broader than expected for quantum confined carriers, exhibiting Hall scattering factors significantly greater than the generally assumed unity value. The interfacial electron mobility and Hall scattering factor are likely to be determined by potential fluctuations arising from a disordered transition layer on the SiC side of the SiO₂/SiC interface. For the MOSFET structures studied, charge trapping at the SiO₂/SiC interface was found to determine the interfacial free electron sheet density, in agreement with prior studies on similar device structures. HR-MSA has enabled unambiguous discrimination between electrons in the ion-implanted buried channel layer and at SiO₂/SiC interface in a depletion-mode MOSFET structure.

Keywords: SiC, MOSFET, mobility spectrum analysis, Hall-effect, mobility distribution, inversion layer

1. Introduction

Silicon carbide (SiC) is regarded as a most promising wide bandgap semiconductor material for the realization of power electronic devices needed to boost output power density and efficiency in power control modules for the next-generation of electrically powered vehicles, promising also significant reductions in module size and weight [1]. In particular, SiC-based power metal-oxide-semiconductor field effect transistors (MOSFETs) are expected to have major applications in alternative energy power converters, motor control, photovoltaics, telecommunications, heating and robotics, and power transmission [1, 2].

Although state-of-the-art SiC-based MOSFETs have demonstrated performance levels superior to those of Si-based devices at similar power ratings, the performance of SiC-based devices is still limited by inversion-layer channel resistance [3, 4]. Post-oxidation annealing has enabled significant reduc-

tions in channel resistance, as well as increased transconductance and reduced trap densities at the SiO₂/SiC interface [4–6]. Although the field-effect mobility is typically employed as a figure of merit to evaluate inversion layer electronic transport, the free electron density in the inversion layer tends to be significantly reduced by trapping at SiO₂/SiC interface states, thus resulting in field-effect mobility values that significantly underestimate the true inversion layer conduction mobility as determined from Hall-effect measurements [4–7]. In this paper, we present results of room-temperature Hall-effect characterization of both normally-on and normally-off 4H-SiC MOSFET structures.

2. Experiment and Sample Details

Lateral n-channel MOS-gated Hall bridge structures with effective active area defined by $L=400$ μm and $W=40$ μm were fabricated on Al-doped p-type epitaxial layers grown on 4° off-axis (0001) Si-face 4H-SiC wafers. Two different samples from the same wafer die were studied: Sample 1, with

¹Corresponding author

channel layer defined in the as-grown p-type epitaxial layer (with nominal acceptor concentration of $5 \times 10^{15} \text{ cm}^{-3}$); and Sample 2, on which a buried n-type layer was formed in the original p-type epilayer through ion-implantation of N-ions with a projected range of 300 nm to an effective donor density of $9 \times 10^{16} \text{ cm}^{-3}$. The gate oxide layer was formed by dry oxidation at 1175 °C, followed by a wet re-oxidation anneal at 950 °C and a 1175 °C 2h post-oxidation anneal in NO. The final oxide thickness was $54 \pm 1 \text{ nm}$.

Magnetic-field dependent resistivity and Hall-effect measurements were performed as a function of applied gate bias at room temperature and magnetic field intensities B up to 12 T. For all measurements, the drain of the Hall bridge structures was biased at $V_{DS}=1 \text{ V}$, which resulted in effective biases as measured at the resistivity probes that did not exceed 0.34 V, whilst the substrate contact to the underlying p-type layer was biased at 0 V. From the measured sheet resistivity R_s and Hall coefficient R_H , the conductivity tensor components σ_{xx} and σ_{xy} were obtained from:

$$\sigma_{xx} = \frac{R_s}{R_s^2 + R_H^2}; \text{ and } \sigma_{xy} = \frac{R_H B}{R_s^2 + R_H^2} \quad (1)$$

which, in principle, contain information about all carriers present in the sample according to the discretized mobility transform equations [8–10]:

$$\sigma_{xx} = \sum_j \frac{S_p(\mu_j) + S_n(\mu_j)}{1 + \mu_j^2 B^2} \quad (2)$$

$$\sigma_{xy} = \sum_j \frac{[S_p(\mu_j) - S_n(\mu_j)] \mu_j B}{1 + \mu_j^2 B^2} \quad (3)$$

where $S_p(\mu) = q \mu p(\mu)$ and $S_n(\mu) = q \mu n(\mu)$ are the hole and electron conductivities in the mobility domain (i.e., the *mobility spectrum*), respectively; $p(\mu)$ and $n(\mu)$ are hole and electron sheet densities, respectively, expressed in terms of their mobility distribution, and q is electronic charge. High-resolution mobility spectrum analysis (HR-MSA) was employed to solve the coupled inverse transform problem posed by Eqs. 2 and 3, and thus extract $S_p(\mu)$ and $S_n(\mu)$ [10]. From the mobility spectra, the sheet carrier concentration N_s and mean mobility μ_D associated with the i -th conductivity peak were calculated from:

$$N_s = \sum_i \frac{S_n(\mu_i)}{q \mu_i}; \text{ and } \mu_D = \frac{1}{q N_s} \sum_i S_n(\mu_i) \quad (4)$$

The mean mobility thus extracted is effectively the drift mobility, since it is an average with respect to the total electron concentration of the i -th peak [10, 11]. The Hall-effect mobility μ_H , defined as the mobility average with respect to the total conductivity of the i -th peak σ_s , is then calculated from:

$$\sigma_s = \sum_i S_n(\mu_i), \text{ and } \mu_H = \frac{1}{\sigma_s} \sum_i \mu_i S_n(\mu_i) \quad (5)$$

From (4) and (5), the Hall scattering factor r_H can then be calculated from:

$$r_H = \frac{\mu_H}{\mu_D} \quad (6)$$

It should be noted that determination of r_H using the above expressions assume that the magnetic field has negligible influence on the carrier mobility distribution.

3. Results and discussion

Extracted inversion layer electron mobility and sheet density for Sample 1 are presented in Fig. 1, where it is evident that the field-effect mobility μ_{FE} (extracted from the MOSFET transconductance) significantly underestimates the mobility of free electrons in the channel as extracted from conventional Hall-effect analysis, or from magnetic-field dependent measurements combined with HR-MSA. This observation, which is consistent with previously reported results [3–5, 7], is attributable to charge trapping at the SiO_2/SiC interface. As illustrated in Fig. 2 for $V_G = 15 \text{ V}$, the inversion layer electron mobility distribution, as extracted from HR-MSA, was found to be relatively broad, indicating a Hall scattering factor r_H significantly greater than the generally assumed unity value [5].

Extraction of transport parameters for Sample 2, a depletion-mode MOSFET (with a deep n-type buried channel layer) in which the gate bias can modulate the electron density near the SiO_2/SiC interface, is significantly more challenging because the sample conductivity is dominated by electron transport in the buried ion-implanted n-type layer. In this case, HR-MSA offered the only means for accurate discrimination of inversion layer transport parameters from those associated with the buried channel layer. The extracted parameters as a function of applied gate bias are summarized in Fig. 3.

As shown by the mobility spectrum for Sample 2 at $V_G = 15 \text{ V}$ in Fig. 4, the mobility of electrons at the SiO_2/SiC interface was found to be

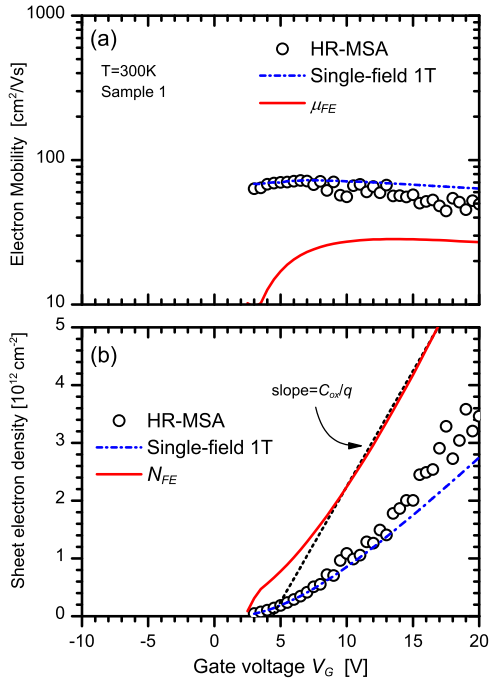


Figure 1: Extracted inversion layer transport parameters for Sample 1: (a) mobility, and (b) sheet electron density, extracted employing different analysis methods: High-resolution mobility spectrum analysis (HR-MSA), conventional Hall-effect analysis at a single magnetic field intensity of 1 T, and field-effect (FE) parameters from gated Hall bridge MOSFET transconductance.

remarkably broad with a significant spread of the electron population towards low mobilities. Inversion layer mobilities were found to be significantly higher in Sample 2 than in Sample 1 at equivalent sheet electron densities, and also exhibited lower r_H values (equivalent to narrower inversion layer electron mobility distribution linewidth). It is noted, however, that for both samples the free electron density near the SiO₂/SiC interface represents less than 50% of the total interfacial sheet electron density N_{total} expected from the ideal charge control model. This result, which is consistent with prior reports [4, 5, 7], suggests that the mobilities should be approximately similar if Coulombic scattering by trapped electrons is the dominant mobility degradation mechanism. In contrast, we observe that interface electrons in Sample 2 have significantly higher mobilities and narrower mobility distribution compared to Sample 1. Given the report of Zheleva *et al.*, on the observation of a disordered transition layer on the SiC side of the SiO₂/SiC interface [12], it is likely that the electron mobility at

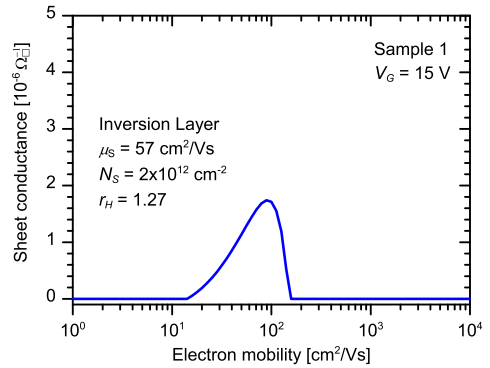


Figure 2: Inversion layer electron mobility spectrum for Sample 1 at $V_G = 15$ V as extracted by HR-MSA from magnetic field dependent measurements.

the SiO₂/SiC interface is determined by scattering processes associated with interfacial potential fluctuations [4, 13], which may lead to electron mobility distributions significantly broader than would be expected for two-dimensionally quantum confined carriers. The interfacial electron mobility enhancement observed in Sample 2 may be due to screening or to reduction of such potential fluctuations by intentional donors arising from the ion-implanted buried channel layer.

Finally, regarding the electronic transport parameters associated with electrons in the ion-implanted buried n-type layer, it can be seen from Fig. 4 that the linewidth of their mobility spectra is significantly narrower, characterized by r_H values < 1.02 for all gate biasing conditions. The approximately gate-bias independent electron mobility of 592 ± 12 cm²/Vs, and Hall scattering factor $r_H < 1.02$, are in excellent agreement with those reported for bulk 4H-SiC at equivalent donor concentrations [14].

4. Summary

Magnetic-field dependent resistivity and Hall-effect measurements combined with high-resolution mobility spectrum analysis have been employed to characterize electronic transport at the SiO₂/SiC interface of 4H-SiC MOSFET structures. It has been shown that the inversion layer electron mobility distribution is significantly broader than expected for quantum confined carriers, exhibiting Hall scattering factors significantly greater than the generally assumed unity value. Interfacial electron

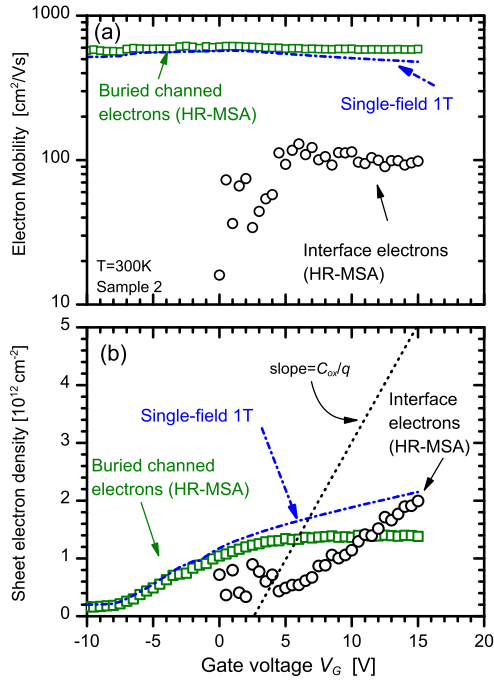


Figure 3: Extracted electron transport parameters for the ion-implanted buried channel and the electron layer at the the SiO₂/SiC interface in Sample 2: (a) mobility, and (b) sheet electron density, extracted employing different analysis methods: HR-MSA, and conventional Hall-effect analysis at 1 T. Conventional Hall-effect analysis yielded average mobility and sheet density approaching those of the dominant ion-implanted buried channel.

mobility and Hall scattering factor are likely to be determined by potential fluctuations arising from a disordered transition layer on the SiC side of the SiO₂/SiC interface. For the MOSFET structures studied, charge trapping at the SiO₂/SiC interface was found to determine the interfacial free electron sheet density, in agreement with prior studies on similar device structures. HR-MSA has enabled the discrimination of inversion and buried channel layer electron transport parameters in a normally-on MOSFET with a deep n-type ion-implanted buried channel layer.

Acknowledgements

This work was supported by the Australian Research Council (DP140103667, FS110200022, LE110100200), the Australian National Fabrication Facility, and the Office of Science of the State Government of Western Australia. The devices investigated were provided under the U.S. Army Research

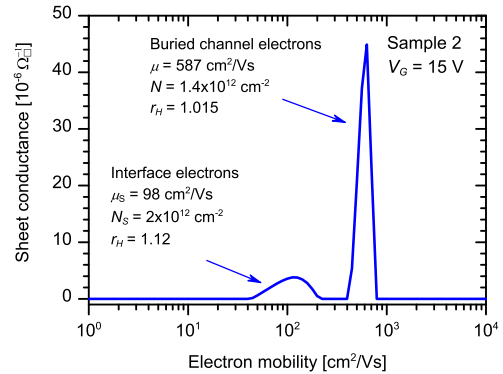


Figure 4: Electron mobility spectrum for Sample 2 at $V_G = 15$ V as extracted by HR-MSA from magnetic field dependent measurements. The broad electron mobility distribution of the electron layer at the the SiO₂/SiC interface is narrower than the spectrum shown in Fig. 2 for Sample 1.

Laboratory's CA #W911NF-04-2-0022 (monitored by Mr. C. Scozzie).

References

- [1] K. Hamada, M. Nagao, M. Ajioka, F. Kawai, IEEE Trans. Electron Devices 62 (2) (2015) 278–285.
- [2] V. Pala, E. Brunt, L. Cheng, M. O'Loughlin, J. Richmond, A. Burk, S. Allen, D. Grider, J. Palmour, C. Scozzie, in: Proc. 2014 IEEE ECCE, 449–454.
- [3] J. Wang, T. Zhao, J. Li, A. Huang, R. Callanan, F. Husna, A. Agarwal, IEEE Trans. Electron Devices 55 (2008) 1798–1806.
- [4] S. Dhar, S. Haney, L. Cheng, S.-R. Ryu, A. K. Agarwal, L. C. Yu, K. P. Cheung, J. Appl. Phys. 108 (2010) 054509.
- [5] N. S. Saks, A. K. Agarwal, Appl. Phys. Lett. 77 (2000) 3281–3283.
- [6] D. Okamoto, H. Yano, K. Hirata, T. Hatayama, T. Fuyuki, IEEE Electron Device Lett. 31 (2010) 710–712.
- [7] G. Ortiz, C. Strenger, V. Uhnevionak, A. Burenkov, A. J. Bauer, P. Pichler, F. Cristiano, E. Bedel-Pereira, V. Mortet, Appl. Phys. Lett. 106 (2015) 062104.
- [8] W. A. Beck, J. R. Anderson, J. Appl. Phys. 62 (1987) 541–554.
- [9] J. Antoszewski, L. Faraone, I. Vurgaftman, J. Meyer, C. Hoffman, J. Electron. Mater. 33 (2004) 673–683.
- [10] G. A. Umana-Membreno, J. Antoszewski, L. Faraone, Microelec. Eng. 109 (2013) 232–235.
- [11] D. Chrastina, J. P. Hague, D. R. Leadley, J. Appl. Phys. 94 (2003) 6583–6590.
- [12] T. Zheleva, A. Lelis, G. Duscher, F. Liu, I. Levin, M. Das, Appl. Phys. Lett. 93 (2008) 022108.
- [13] T. Ouisse, phys. stat. sol. (a) 162 (1997) 339–368.
- [14] S. Kagamihara, H. Matsuura, T. Hatakeyama, T. Watanabe, M. Kushibe, T. Shinohe, K. Arai, J. Appl. Phys. 96 (2004) 5601–5606.